High-performance organic semiconductors for thin-film transistors based on 2,7-divinyl[1]benzothieno[3,2-*b*]benzothiophene†

Myoung-Chul Um,[a] Jeonghun Kwak,[b] Jung-Pyo Hong,[a] Jihoon Kang,[a] Do Yeung Yoon,[a] Seong Hoon Lee,[a] Changhee Lee*[b] and Jong-In Hong*[a]

Received 19th May 2008, Accepted 10th July 2008
First published as an Advance Article on the web 27th August 2008
DOI: 10.1039/b808438f

We have synthesized two novel organic semiconductors, which have a symmetrically substituted 2,7-divinyl[1]benzothieno[3,2-*b*]benzothiophene backbone. They show good electrical performances on a SiO_2/Si substrate, with high field-effect mobilities of up to 0.4 $cm^2\ V^{-1}\ s^{-1}$, and can easily be synthesized in large quantities. In addition, there is no significant change in the mobility of DPV-BTBT even after the device is exposed to air for at least 60 days (further monitoring is in progress), showing that it is a promising air-stable p-channel organic semiconductor that can be applied to all-organic flexible electronic devices.

Introduction

Conjugated organic materials are of tremendous interest because of their potential use as organic semiconductors for various optoelectronic devices, some of which include organic thin-film transistors (OTFTs),[1–3] organic light-emitting diodes (OLEDs),[4] photovoltaic cells,[5] sensors,[6] and radio-frequency identification (RF-ID) tags.[7] The design and synthesis of new conjugated organic semiconductors have attracted significant research interest in the past decade. In particular, π-extended heteroarenes containing chalcogenophenes (*i.e.*, thiophene and/or selenophene) in fused aromatic ring systems have been actively investigated because of their structural resemblance to oligoacenes.[8] Currently, the mobilities of the charge carriers in organic semiconductors have outperformed the mobility of amorphous silicon (0.5 $cm^2\ V^{-1}\ s^{-1}$), *i.e.*, 2,7-diphenyl[1]benzothieno[3,2-*b*]benzothiophene (DPh-BTBT): ~2.0 $cm^2\ V^{-1}\ s^{-1}$; 2,7-diphenyl[1]benzoselenopheno[3,2-*b*]benzobenzoselenophene (DPh-BSBS):[8a] ~0.3 $cm^2\ V^{-1}\ s^{-1}$; dinaphtho[2,3-*b*:2′,3′-*f*]chalcogenopheno[3,2-*b*]chalcogenophene (DNTT and DNSS): ~2.9 and ~1.0 $cm^2\ V^{-1}\ s^{-1}$.[9] These compounds were recently reported to be high-performance OTFT materials with reasonable stabilities when operated under ambient conditions. In addition, very recently, several research groups have developed semiconductors with high stabilities and conductivities by employing conjugated vinylene-based oligomers.[10] In fact, the presence of a double bond of a defined configuration has been found to result in a reduction in the overall aromatic character of the planar structures, and hence an increase in the π-electron localization.[11] The introduction of a vinylene unit into π-conjugated oligomeric structures is a well-known method for forming coplanar molecules with an extended π-conjugated length, which should help maximize the organization of the molecules in thin films. Devices derived from vinylene-substituted compounds such as 2,6-bis[2-(phenyl)vinyl]anthracene (DPVAnt) not only show very high field-effect mobilities (up to 1.3 $cm^2\ V^{-1}\ s^{-1}$) and on/off ratios (up to 10^7) but are also found to be exceptionally long-lived and stable even when continuously operated under atmospheric conditions.[12] In addition, OTFT devices derived from 2,6-bis[2-(4-pentylphenyl)vinyl]anthracene (DPPVAnt) also showed high mobilities (0.1–1.28 $cm^2\ V^{-1}\ s^{-1}$) and on/off ratios (10^6–10^7).[13] However, there are still very few organic semiconductors endowed with both high durability and high OTFT performance. Hence, there is a demand for new semiconductor materials that have both high mobilities and high durabilities.

With the above consideration in mind, we focused our attention on π-conjugated heteroarene cores with vinyl groups (DCV-BTBT and DPV-BTBT, Fig. 1) as new promising organic semiconductors.

Experimental

General

The ^1H and ^{13}C NMR spectra were recorded in $CDCl_3$ and DMSO-d_6 using an Advance 300 MHz Bruker spectrometer. The ^1H NMR and ^{13}C NMR chemical shifts in $CDCl_3$ were reported relative to those in $CHCl_3$ (7.27 ppm and 77.23 ppm, respectively).

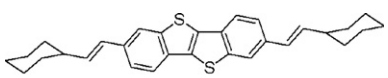

DCV-BTBT

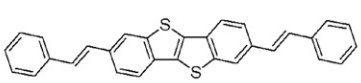

DPV-BTBT

Fig. 1 Structures of DC(P)V-BTBT.

[a]*Department of Chemistry, College of Natural Sciences, Seoul National University, Seoul, 151-747, Korea. E-mail: jihong@snu.ac.kr; Fax: +82-2-889-1568; Tel: +82-2-880-6682*
[b]*School of Electrical Engineering and Computer Science, Seoul National University Kwanak, P.O. Box 34, Seoul, 151-600, Korea. E-mail: chlee7@snu.ac.kr; Fax: +82-2-872-6451; Tel: +82-2-880-955*

† Electronic supplementary information (ESI) available: CV, UV, PL, AFM, XRD and more detailed device data. See DOI: 10.1039/b808438f

Physical measurements

The TGA analyses were performed on a TGA Q50 TA instrument at 10 °C min^{-1} under a nitrogen atmosphere. The DSC analyses were performed on a DSC2910 TA instrument at 10 °C min^{-1} under nitrogen flow. The UV-vis absorption spectra were recorded on a Beckman Coulter DU 800 spectrophotometer using quartz cells with path lengths of 2.5 cm. For solid-state measurements, the oligomers were thermally evaporated in a vacuum chamber on quartz plates to form 300 Å-thick films at a deposition rate of 0.5 Å s^{-1}. The XRD analyses were carried out at room temperature with a Mac Science (M18XHF-22) diffraction meter using CuKα radiation as the X-ray source at 50 kV and 100 mA. The data were collected in the conventional θ–2θ configuration (2.5–30°) from thin films thermally evaporated on SiO_2/Si substrates in a vacuum chamber to form 300 Å-thick films at a rate of 0.5 Å s^{-1}. The AFM images of the vacuum-deposited thin films were recorded using a PSIA XE-100 Advanced Scanning Microscope. The voltammetric apparatus used was a CH Instruments model 700C electrochemical workstation. The cyclic voltammograms (CVs) were obtained at room temperature in a three-electrode cell equipped with a working electrode (Au), a reference electrode (Ag/AgCl), and a counter electrode (Pt) in dichlorobenzene containing tetrabutylammonium hexafluorophosphate ($Bu_4N^+PF_6^-$, 0.1 M) as the supporting electrolyte at a scan rate of 100 mV s^{-1}. All the potentials were calibrated with the standard ferrocene/ferrocenium redox couple (E = + 0.41 V measured).

Fabrication of TFT devices

The field-effect measurements were carried out using top-contact FETs. TFT devices with a channel length (L) of 50 μm and a channel width (W) of 1000 μm were fabricated on thermally oxidized highly n-doped silicon substrates. The SiO_2 gate dielectric was 300 nm in thickness. The organic semiconductor (300 Å) was evaporated (0.1 Å s^{-1} at 1 × 10^{-6} Torr) onto a non-pretreated or octadecyltrichlorosilane (OTS)-pretreated oxide surface. Gold source/drain electrodes were evaporated on top of the films through a shadow mask. All the measurements were performed at room temperature using a 4155C Agilent semiconductor parameter analyzer, and the mobilities (μ) were calculated in the saturation regime by using the relationship $\mu_{sat} = (2I_{DS}L)/(WC(V_g - V_{th})^2)$, where I_{DS} is the source–drain saturation current; C (1.18 × 10^{-8} F), the oxide capacitance; V_g, the gate voltage; V_{th}, the threshold voltage.

Synthesis

2,7-Dihydroxymethyl[1]benzothieno[3,2-*b*]benzothiophene. To a solution of [1]benzothieno[3,2-*b*]benzothiophene-2,7-dicarboxylate (1.50 g, 3.9 mmol) in THF (40 mL) was added $LiAlH_4$ (0.74 g, 19.5 mmol). The reaction mixture was stirred overnight. The insoluble material was removed by filtration and washed with hot DMSO. The filtrate and washings were collected, and the product was precipitated by adding 50 mL of 1 N HCl. The product was collected by filtration to afford 1.86 g (75%) of pure 2,7-dihydroxymethyl[1]benzothieno[3,2-*b*]benzothiophene. ^{1}H NMR (300 MHz, DMSO-d_6): δ 8.05 (s, 2H), 7.98 (d, 2H, J = 8.1 Hz), 7.48 (d, 2H, J = 8.2 Hz), 5.38 (t, 2H, J = 5.6 Hz), 4.69 (d, 4H, J = 5.3 Hz).

2,7-Dibromomethyl[1]benzothieno[3,2-*b*]benzothiophene. Phosphorus tribromide (3.24 g, 11.9 mmol) was added dropwise to a suspension of 2,7-dihydroxymethyl[1]benzothieno[3,2-*b*]benzothiophene (0.9 g, 2.99 mmol) in DMF (20 mL) at 0 °C. Upon the formation of a yellow precipitate, the mixture was warmed to room temperature and stirred for 4 h. The solids were collected by filtration and were washed with water and hexane to afford 2,7-dibromomethyl[1]benzothieno[3,2-*b*]benzothiophene as a yellow solid (1.1 g, 78%). The product was further purified by recrystallization from DMF. ^{1}H NMR (300 MHz, DMSO-d_6): δ 8.24 (s, 2H), 8.08 (d, 2H, J = 8.2 Hz), 7.63 (d, 2H, J = 8,1 Hz), 4.91 (s, 4H).

2,7-Bis(diethylphosphorylmethyl)[1]benzothieno[3,2-*b*]benzothiophene. 2,7-Dibromomethyl[1]benzothieno[3,2-*b*]benzothiophene (1.1 g, 2.58 mmol) was added to triethylphosphite (30 mL), and the resulting solution was refluxed for 12 h. The solvent was removed *in vacuo*, and the residue was purified by column chromatography on silica gel using ethyl acetate–dichloromethane (2 : 1) as the eluent to obtain the product in 90% yield. ^{1}H NMR (300 MHz, $CDCl_3$): δ 7.87 (s, 2H), 7.84 (d, 2H, J = 8.2 Hz), 7.42 (d, 2H, J = 8.1 Hz), 4.05 (m, 8H), 3.36 (d, 4H, J = 21.5 Hz), 1.27 (t, 12H, J = 7.0 Hz). ^{13}C NMR (75 MHz, $CDCl_3$): (142.62, 142.58), 133.18, 131.90, (128.79, 128.67), (126.92, 126.84), (124.98, 124.88), 121.40, (62.33, 62.24), (34.81, 32.97), (16.45, 16.37).

2,7-Bis(2-cyclohexylvinyl)[1]benzothieno[3,2-*b*]benzothiophene (DCV-BTBT). LDA (1.5 M in cyclohexane, 4.0 mL, 6.0 mmol) was added dropwise to a stirred solution of 2,7-bis(diethylphosphorylmethyl)[1]benzothieno[3,2-*b*]benzothiophene (1.3 g, 2.41 mmol) in anhydrous THF (50 mL) at −78 °C under a nitrogen atmosphere. The mixture was stirred for 1 h, and then cyclohexanecarbaldehyde (0.67 g, 6.02 mmol) in THF (10 mL) was added dropwise over a period of 10 min. After the mixture was stirred for 2 h at −78 °C and for 12 h at room temperature, 5 mL of water was added, and the solvent was evaporated off. The residue was washed with water and MeOH. The desired product was separated by sublimation (0.77 g, 70%). High-resolution mass spectrometry (HRMS): Calcd for $C_{30}H_{32}S_2$: 456.1945. Found: 456.1951. Anal. Calcd for CHS: C, 78.90; H, 7.06; S, 14.04. Found: C, 78.48; H, 7.14; S, 14.36%.

2,7-Distyryl[1]benzothieno[3,2-*b*]benzothiophene (DPV-BTBT). LDA (1.5 M in cylohexane, 4.0 mL, 6.0 mmol) was added dropwise to a stirred solution of 2,7-bis(diethylphosphorylmethyl)[1]benzothieno[3,2-*b*]benzothiophene (1.3 g, 2.41 mmol) in anhydrous THF (50 mL) at −78 °C under a nitrogen atmosphere. The mixture was stirred for 1 h, and then benzaldehyde (0.67 g, 6.0 mmol) in THF (20 mL) was added dropwise over a period of 10 min. After the mixture was stirred for 2 h at −78 °C and for 12 h at room temperature, 5 mL of water was added, and the solvent was evaporated off. The residue was washed with water and MeOH. The desired product was separated by sublimation (0.68 g, 64%). HRMS: Calcd for $C_{30}H_{20}S_2$: 444.1006. Found: 444.1008. Anal. Calcd

For CHS: C, 81.04; H, 4.53; S, 14.42. Found: C, 81.04; H, 4.55; S, 14.40%.

Results and discussion

Although there are several possible synthetic approaches to the target compounds, we selected the Horner–Emmons coupling reaction between phosphonates and aldehyde derivatives for introducing vinyl groups, as shown in Scheme 1. The Horner–Emmons coupling reaction is well known for yielding products with all-*trans* configurations.[14] The synthetic route for the preparation of DCV-BTBT and DPV-BTBT is presented in Scheme 1. The synthesis of the [1]benzothieno[3,2-*b*]benzothiophene-2,7-dicarboxylate was carried out from 2,2′-diamino-(*E*)-stilbene-4,4′-dicarboxylate, which was prepared as already reported.[15a] The entire procedure for the conversion to DCV-BTBT and DPV-BTBT consists of ten steps. First, commercially available 4-(chloromethyl)benzoic acid was converted into its ethyl ester and nitrated to yield ethyl 4-(chloromethyl)-3-nitrobenzoate. Two of the ester molecules were then condensed to afford diethyl 2,2′-dinitro-(*E*)-stilbene-4,4′-dicarboxylate by treatment with sodium ethoxide. The nitro groups were reduced using iron powder in ethanol in the presence of hydrochloric acid to give diethyl 2,2′-diamino-(*E*)-stilbene-4,4′-dicarboxylate. The amino groups so formed were converted into xanthate groups *via* a bisdiazonium salt. Treatment of the stilbene bisxanthate with bromine in acetic acid yielded the fused thiophene ring, diethyl[1]benzothieno[3,2-*b*]benzothiophene-2,6-dicarboxylate, which was then reduced with $LiAlH_4$ in THF to afford 2,7-dihydroxymethyl[1]benzothieno[3,2-*b*]benzothiophene in good yield. Treatment of the resulting diol with phosphorus tribromide in DMF at room temperature afforded 2,7-dibromomethyl[1]benzothieno[3,2-*b*]benzothiophene. One of the precursors of the Horner–Emmons olefination, 2,7-diethylphosphorylmethyl[1]benzothieno[3,2-*b*]benzothiophene, was prepared by the reaction of the dibromide with triethylphosphite. The organization of oligomers in thin films can be maximized by the introduction of vinylene units. The final step of the conversion was accomplished by Horner–Emmons coupling reactions between the phosphonate and the aldehyde derivatives, as shown in Scheme 1. After purification by sublimation, DCV-DTBT and DPV-BTBT were identified by HRMS and elemental analyses. The thermal stabilities of DCV-DTBT and DPV-BTBT were investigated by thermal gravimetric analysis (TGA). The TGA analysis showed that DPV-BTBT is thermally more stable than DCV-BTBT, probably due to the difference between the thermal stabilities of the phenyl and cyclohexane groups. The thermal decomposition temperatures were observed to be 347 °C for DCV-DTBT and 400 °C for DPV-BTBT while, by contrast, pentacene began to decompose at 260 °C (due to sublimation), indicating that DC(P)V-DTBT compounds have high thermal stabilities (Fig. 2).

The DSC results reveal the melting features of the two materials. In the case of DCV-BTBT, an endothermic transition and an exothermic transition were observed at temperatures at 301

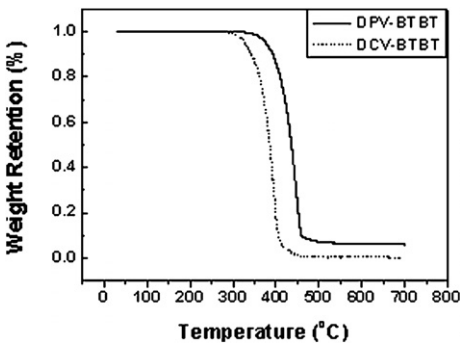

Fig. 2 Thermal gravimetric analysis (TGA) of DC(P)V-BTBT.

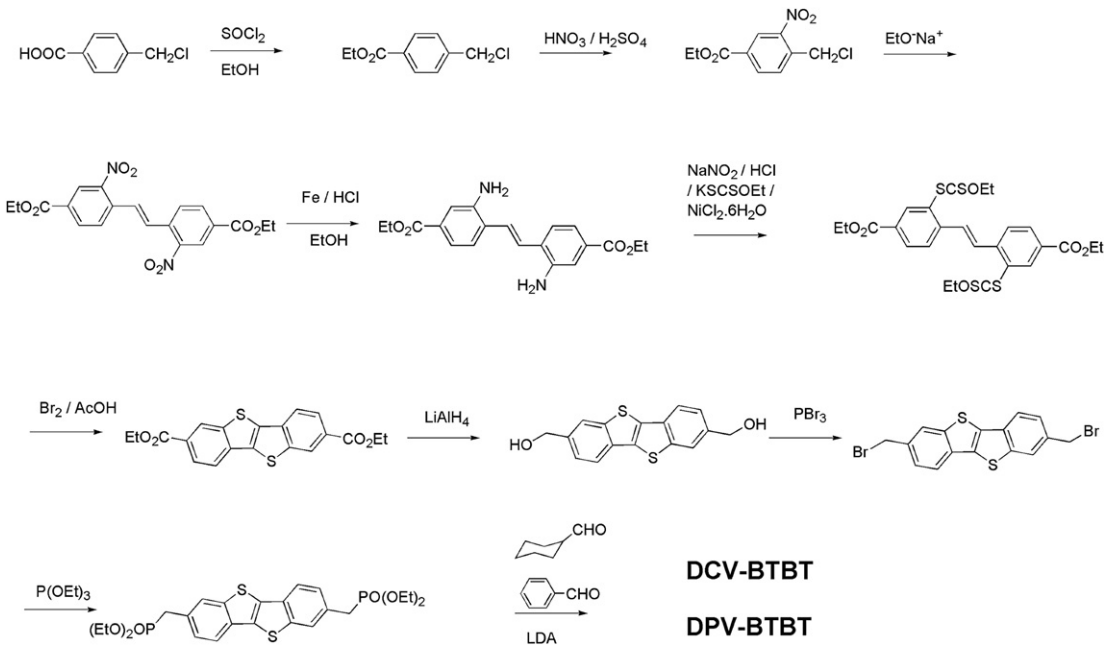

Scheme 1 Synthesis of DC(P)V-BTBT.

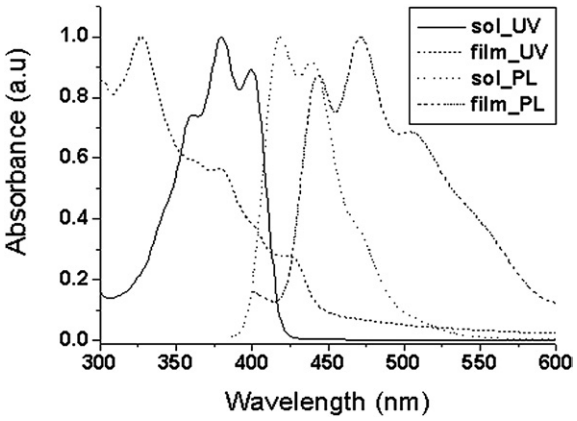

Fig. 3 UV-vis absorption spectra of DPV-BTBT.

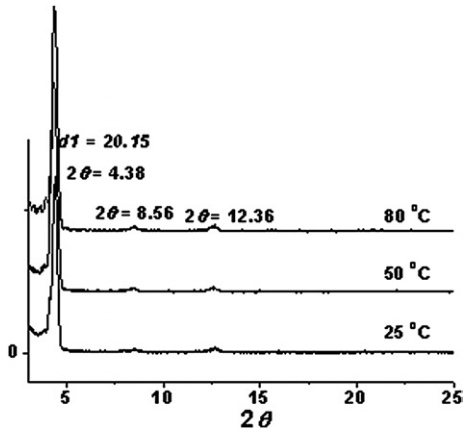

Fig. 4 XRD patterns of DPV-BTBT thin films vacuum-deposited on OTS-treated SiO_2/Si at T_{sub} = 25, 50, and 80 °C.

°C (56.00 J g^{-1}) and 255 °C (41.29 J g^{-1}), respectively, during the heating and cooling cycles. On the other hand, DPV-BTBT was observed to have two endothermic peaks at 325 °C (35.87 J g^{-1}) and 352 °C (58.63 J g^{-1}). In the cooling trace, only one exothermic peak at 330 °C (47.84 J g^{-1}) was observed.

The UV-vis spectrum of a dilute solution of DPV-BTBT in xylene showed absorption peaks at 399, 379, and 359 nm (Fig. 3). It is generally recognized that an increase in the planarity of conjugated systems leads to a decrease in the HOMO–LUMO gap and a corresponding red shift of the absorption spectra. The long-wavelength absorptions in the UV-vis spectrum of the DPV-BTBT solution showed greater red shifts (38 nm) than those in the UV-vis spectrum of the DCV-BTBT solution. The DPV-BTBT films showed a greater blue shift of their main absorption peaks as compared to those of their diluted xylene solutions, which suggests H-aggregate formation by analogy with previous studies.[15b,c] Interestingly, in the PL spectra, the differences in the emission maxima between the solution and film states of DCV-BTBT and DPV-BTBT were 47 and 60 nm, respectively, indicating the presence of extremely strong intermolecular interactions in the film states.[16]

The UV-vis spectra of DCV-BTBT and DPV-BTBT showed long-wavelength absorption edges at 379 and 419 nm, respectively, which corresponded to HOMO–LUMO energy gaps of 3.25 and 2.97 eV, respectively; these values were significantly higher than the energy gap of pentacene (2.2 eV).[17] The HOMO–LUMO energy gap decreases with an increase in the π-conjugation length.

Further insight into the electronic properties of these compounds was provided by cyclic voltammetry (CV). The CV measurements of DCV-BTBT and DPV-BTBT in 0.1 M $Bu_4N^+PF_6^-$/dichlorobenzene solution showed an irreversible oxidation peak. The onset oxidation potentials were 0.69 eV and 0.76 eV *vs.* ferrocene (FOC). With respect to the energy level of the FOC/ferrocenium reference (−4.8 eV), the HOMO energy levels of DCV-BTBT and DPV-BTBT were −5.49 and −5.56 eV, respectively, which were lower than that of pentacene, thus indicating their high oxidative stability (ESI† Fig. S5).[18] The morphological characteristics were investigated by X-ray diffraction (XRD) (Fig. 4 and ESI† Fig. S6).

The thin-film XRD pattern of DPV-BTBT displayed a primary diffraction peak at $2\theta = 4.38°$ (*d*-spacing: 20.15 Å), with second- and third-order diffraction peaks at $2\theta = 8.56°$ and 12.36°, respectively. The strong intensity of the X-ray diffraction peaks indicated the formation of lamellar ordering and crystallinity on the substrate. The *d*-spacing of DPV-BTBT obtained from the first reflection peak was 20.15 Å, which was comparable to the molecular length obtained from the MM2 calculation (22.42 Å). These spacings were consistent with the monomolecular layer thickness obtained by atomic force microscopy (AFM), as shown in Fig. 7 (later) and Fig. S3 (ESI†), which indicated a near-perpendicular alignment of the molecules with respect to the substrate surface. In contrast, the XRD results of the DCV-BTBT films exhibited very weak reflection peaks. This may be attributed to the unique molecular stacking structure of DCV-BTBT, where a molecular layer structure is not well formed along the molecular long axis. It is assumed that the weak reflection peaks of DCV-BTBT have a negative effect on the mobility of the OFETs. This assumption is also in agreement with the performance of the devices. When used as a channel semiconductor in OTFTs, DCV-BTBT provided lower FET mobility than DPV-BTBT. XRD measurements at higher substrate temperatures of DCV-BTBT thin films vacuum-deposited on OTS-treated SiO_2/Si did not show increased reflection peaks.

Thin films of the two conjugated oligomers were formed by vacuum evaporation onto either untreated or OTS-coated Si/SiO_2 substrates at various temperatures (T_{sub} = 25 °C, 50 °C and 80 °C). All the OTFTs showed typical p-channel TFT characteristics. The OTFTs of DCV-BTBT and DPV-BTBT were fabricated with Au electrodes using top-contact geometry. Gold source and drain contacts (50 nm) were deposited onto the organic layer through a shadow mask. The channel length (*L*) and width (*W*) were 50 μm and 1000 μm, respectively.

Fig. 5 shows the plot of the drain current (I_{DS}) versus drain-source voltage (V_{DS}) and the transfer characteristics of DPV-BTBT TFTs grown at a substrate temperature (T_{sub}) of 80 °C. From the electrical transfer characteristics, we estimated several parameters such as the carrier mobility, on/off current ratio, threshold voltage, and subthreshold swing for each device. These are summarized in Table 1. We have demonstrated that a high carrier mobility can be obtained with DPV-BTBT even after the devices had been exposed to air for 2 months (Fig. 5).

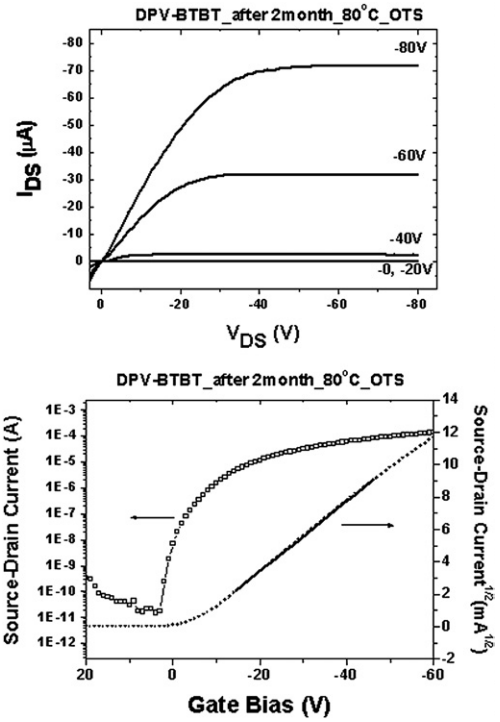

Fig. 5 Source–drain current (I_{DS}) *versus* source–drain voltage (V_{DS}) at various gate voltages (V_G) for top-contact field-effect transistor using DPV-BTBT deposited at $T_{sub} = 80$ °C on OTS-treated SiO_2. The transfer characteristics in the saturation regime at a constant source–drain voltage ($V_{DS} = -100$ V) are also included.

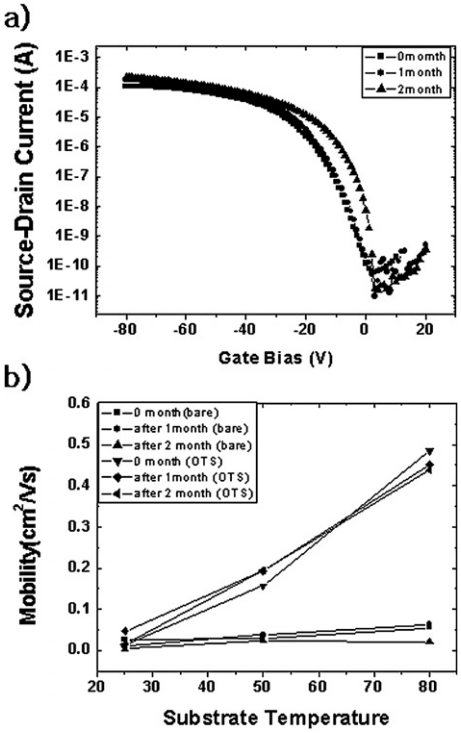

Fig. 6 a) The transfer characteristics in the saturation regime at a constant source–drain voltage ($V_{DS} = -100$ V) with different times. b) OTFT hole mobilities of DPV-BTBT were collected under ambient conditions at different times and substrate temperatures.

Table 1 Field-effect mobility (μ_{TFT}), on/off current ratio (I_{on}/I_{off}), threshold voltage (V_{th}), and subthreshold swing (S) of DPV-BTBT vacuum-deposited on differently treated SiO_2 surfaces and at different substrate temperatures (T_{sub}) after 2 months

SiO_2 surface	T_{sub}	μ_{TFT}/cm^2 V^{-1} s^{-1}	I_{on}/I_{off}	V_{th}/V	S/V decade^{-1}
Bare	25	0.003	10^5	−5.5	2.7
	50	0.024	10^6	−8.8	2.0
	80	0.021	10^7	−7.0	1.8
OTS-treated	25	0.015	10^5	−3.5	1.7
	50	0.244	10^6	−5.7	1.2
	80	0.437	10^7	−4.4	0.9

The DPV-BTBT devices fabricated under various conditions showed μ_{FET} in the range of 0.003–0.437 cm^2 V^{-1} s^{-1} and on/off ratios of $>10^5$–10^7 under ambient conditions (Table 1). In particular, excellent FET characteristics with μ_{FET} higher than 0.437 cm^2 V^{-1} s^{-1} (measured in the saturation regime) and on/off ratios of $>10^5$ were observed in DPV-BTBT devices fabricated on the OTS-treated substrate at $T_{sub} = 80$ °C. As evident from Fig. 6, the mobility of DPV-BTBT showed negligible changes even after 60 days of operation in air (further monitoring is in progress). This observed trend clearly suggests that 2,7-bis(vinyl) BTBT with a lower HOMO level tends to exhibit better air stability.

We found that the TFT performance depends critically on the side-end group of the active materials. Typically, the addition of bulky substituents such as cyclohexyl groups to the ends of the oligomer is expected to increase its solubility, and thus enhance the solution processing.[19]

In our studies, however, we found that DCV-BTBT is not sufficiently soluble in any organic solvent. Moreover, optical microscopic observations revealed that films of cyclohexyl-substituted vinyl-BTBT did not have a continuous morphology

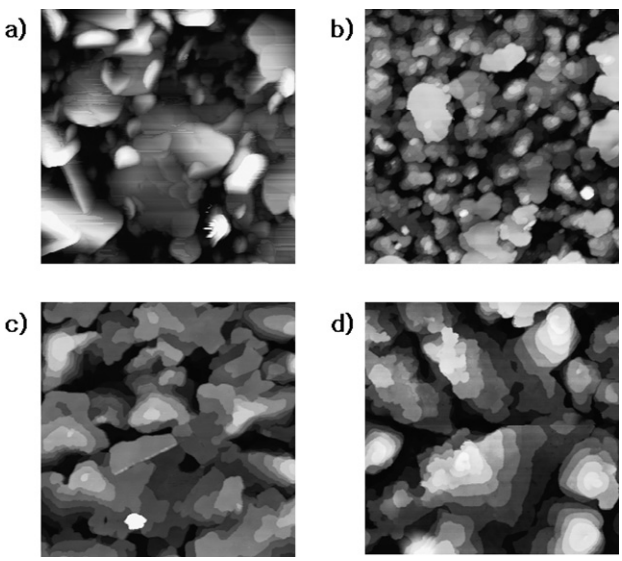

Fig. 7 AFM topography image of 30 nm thin films of DPV-BTBT deposited on OTS treated SiO_2 at various substrate temperatures: a) 25 °C; b) 50 °C; c) 80 °C; and d) 100 °C (2 × 2 μm area).

(ESI† Fig. S4). The mobility of DPV-BTBT was 20 times higher than that of DCV-BTBT. When used as a channel semiconductor in OTFTs, DCV-BTBT exhibited lower FET mobility than DPV-BTBT. This is not surprising since the charge transport in organic semiconductors is dominated by the crystal structure, and thus the less-ordered DCV-BTBT would not be expected to exhibit a high mobility (0.024 $cm^2 V^{-1} s^{-1}$, ESI† Fig. S1).[20]

Fig. 7 shows the AFM images of 30- nm-thick films of DPV-BTBT deposited on OTS-treated SiO_2/Si at 25, 50, 80 and 100 °C. At 80 °C, the molecules become more ordered, and a network of interconnected grains can be observed in the DPV-BTBT sample. The AFM step heights for the lamellar structure of the DPV-BTBT grains (as obtained from the films deposited at 80 °C) correspond well to the *d*-spacing obtained from XRD and the calculated molecular length (ESI† Fig. S3).

Conclusions

In summary, a series of substituted vinyl-BTBT molecules were synthesized by a route involving the Horner–Emmons coupling reaction. The oligomers show high thermal stability. DPV-BTBT exhibits excellent field-effect performances, with a mobility as high as 0.46 and an on/off ratio of up to 1.2×10^7. It is notable that the mobility of DPV-BTBT does not significantly change even after the device has been exposed to air for at least 60 days (further monitoring is in progress), showing that it is a promising air-stable p-channel organic semiconductor for application in all-organic flexible electronic devices.

We are currently investigating the OTFT devices based on DCV-BTBT and DPV-BTBT for improving their performances. In addition, we are attempting the introduction of other alkyl chains into DCV-BTBT and DPV-BTBT for the synthesis of new soluble oligomers.

Acknowledgements

This work was supported by grants (F0004030-2007-23, F0004071-2007-23) from the Information Display R&D Center, one of the 21st Century Frontier R&D Program funded by the Ministry of Commerce, Industry, and Energy of the Korean Government, and Seoul R&BD.

References

1 M. H. Yoon, S. A. DiBenedetto, A. Facchetti and T. J. Mark, *J. Am. Chem. Soc.*, 2006, **128**, 9598.
2 K. Takimiya, Y. Kunugi, Y. Konda, H. Ebata, Y. Toyoshima and T. Otsubo, *J. Am. Chem. Soc.*, 2006, **128**, 3044.
3 C. D. Dimitrakopoulos and R. L. Malenfant, *Adv. Mater.*, 2002, **14**, 99.
4 R. H. Friend, R. W. Gymer, A. B. Holmes, J. H. Burrouhes, R. N. Marks, C. Taliani, D. D. C. Bardley, D. A. DosSantos, J. L. Bredas, M. Logdlund and W. R. Salanek, *Nature*, 1999, **397**, 121.
5 (*a*) C. J. Brabec, N. S. Sariciftci and J. C. Hummelen, *Adv. Funct. Mater.*, 2001, **11**, 15; (*b*) K. M. Coakley and M. D. McGhee, *Chem. Mater.*, 2004, **16**, 4533.
6 (*a*) B. Crone, A. Dodabalapur, Y.-Y. Lin, R. W. Filas, Z. Bao, A. LaDuca, R. Sarpeshkar, H. E. Katz and W. Li, *Nature*, 2000, **403**, 521; (*b*) Y.-Y. Lin, A. Dodabalapur, R. Sarpeshkar, Z. Bao, W. Li, K. Baldwin, V. R. Raju and H. E. Katz, *Appl. Phys. Lett.*, 1999, **74**, 2714.
7 (*a*) A. T. Brown, A. Pomp, C. M. Hart and D. M. Deleeuw, *Science*, 1995, **270**, 972; (*b*) C. J. Drury, C. M. Mutsaers, C. M. Hart, M. Matters and D. M. de Leeuw, *Appl. Phys. Lett.*, 1998, **73**, 108.
8 (*a*) K. Takimiya, H. Ebata, K. Sakamoto, T. Izawa, T. Otsubi and Y. Kanug, *J. Am. Chem. Soc.*, 2006, **128**, 12604; (*b*) K. Takimiya, Y. Kunugi, Y. Konda, H. Ebata, Y. Toyoshima and T. Otsubo, *J. Am. Chem. Soc.*, 2006, **128**, 3044; (*c*) H. Ebata, E. Miyazaki, T. Yamamoto and D. Takimiya, *Org. Lett.*, 2007, **9**, 4499; (*d*) H. Ebata, T. Izawa, E. Miyazaki, D. Takimiya, M. Ikeda, H. Kuwabara and T. Yui, *J. Am. Chem. Soc.*, 2007, **129**, 15732.
9 T. Yamamoto and D. Takimiya, *J. Am. Chem. Soc.*, 2007, **129**, 2224.
10 (*a*) M.-C. Um, J. J. Jang, J.-P. Hong, D. Y. Yoon, S. H. Lee, J.-J. Kim and J.-I. Hong, *J. Mater. Chem.*, 2008, **18**, 2234; (*b*) N. Drolet, J. F. Morin, N. Leclerc, S. Wakim, Y. Tao and M. Leclerc, *Adv. Funct. Mater.*, 2005, **15**, 1671; (*c*) T. C. Gorjanc, I. Levesque and M. D'lori, *Appl. Phys. Lett.*, 2004, **84**, 930; (*d*) H. Klauk, U. Zschieschang, R. T. Weitz, H. Mong, F. Sun, G. Nunes, D. E. Keys, C. R. Fincher and Z. Xiang, *Adv. Mater.*, 2007, **19**, 3882.
11 (*a*) G. Distefano, M. Da Colle, D. Jones, M. Zambianchi, L. Favvafetto and A. Modelli, *J. Phys. Chem.*, 1993, **97**, 3504; (*b*) E. Orti, P. M. Viruela, J. Sanchez-Marin and F. Tomas, *J. Phys. Chem.*, 1995, **99**, 4955; (*c*) J. Roncali, *Chem. Rev.*, 1997, **97**, 173.
12 C. Videlot-Ackermann, J. Ackermann, H. Brisset, K. Kawamura, N. Yoshimoto, P. Raynal, A. EI Dassmi and F. Fages, *J. Am. Chem. Soc.*, 2005, **127**, 16346.
13 H. Meng, F. Sun, M. B. Goldfinger, F. Gao, D. J. Londono, W. J. Marshal, G. S. Blackman, D. D. Dobbs and D. E. Keysa, *J. Am. Chem. Soc.*, 2006, **128**, 9304.
14 S. Pfeiffer and H. H. Horhold, *Macromol. Chem. Phys.*, 1998, **200**, 1870.
15 (*a*) P. Kaszynski and D. A. Dougherty, *J. Org. Chem.*, 1993, **58**, 5209; (*b*) F. Nuesh and M. Gratzel, *Chem. Phys.*, 1995, **193**, 1; (*c*) H. Meng, J. Zheng, A. J. Lovinger, B.-C. Wang, P. G. V. Patten and A. Bao, *Chem. Mater.*, 2003, **15**, 1778.
16 J. H. Park, D. S. Chung, J. W. Park, T. Ahn, H. Kong, Y. K. Jung, J. Lee, M. H. Y, C. E. Park, S. K. Kwon and D. D. Shim, *Org. Lett.*, 2007, **9**, 2573.
17 I. G. Hill, J. Hwang, A. Kahn, C. Hung and J. E. McDermott, *Appl. Phys. Lett.*, 2007, **90**, 012109.
18 M. S. Liu, Y. Liu, R. C. Urian, H. Ma and A. K-Y. Jen, *J. Mater. Chem.*, 1999, **9**, 2201.
19 J. Locklin, D. Li, S. C. B. Mannsfeld, E.-J. Borkent, H. Meng, R. Advincula and Z. Bao, *Chem. Mater.*, 2005, **17**, 3366.
20 Y. Wu, Y. Li, S. Gardner and B. S. Ong, *J. Am. Chem. Soc.*, 2005, **127**, 614.